Supplementary information for

Enhanced Electron Collection in a Particulate $LaTiO_2N$ Photoanode for Photoelectrochemical Water Splitting

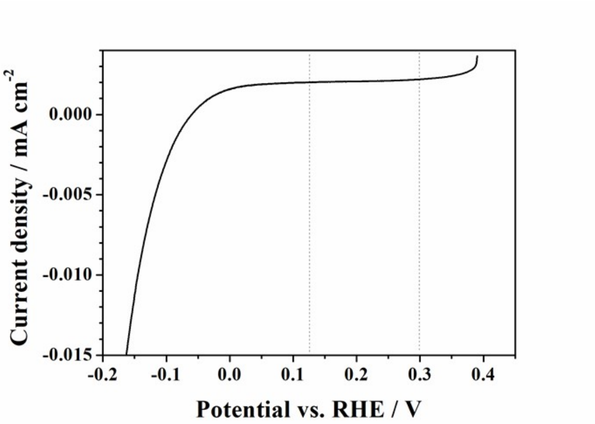

Fig. S1 Current-potential characteristics of the $LaTiO_2N$(as) particle electrodes on Al substrates. The two dotted lines show the potential range where there is only capacitive charging current but no Faraday current, which is used for Mott-Schottky plots.

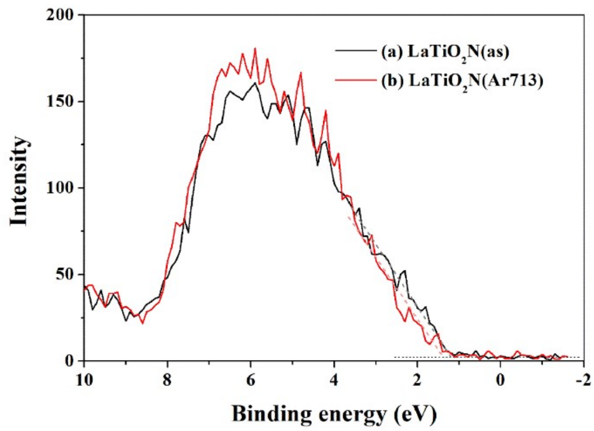

Fig. S2 X-ray photoelectron spectra of valence band of (a) as-prepared $LaTiO_2N$; (b) $LaTiO_2N$ treated in Ar at 713 °C.

The valence band (VB) X-ray photoelectron spectra were obtained with 60 scans on an X-ray photoelectron spectrometer (ESCALAB250Xi, Al K_α, 1486.6 eV) using contamination C1s (284.8 eV) for the calibration. The significant increase of electron carrier density in the bulk would elevate the position of Fermi level relative to the top of valence band. As shown by valence band X-ray photoelectron spectra, the binding energy at valence band edge is increased somewhat for $LaTiO_2N$(Ar713) compared with $LaTiO_2N$(as). This indicates that the distance between the Fermi level and the valence band top is increased, which is consistent with the results of Mott-Schottky analysis.

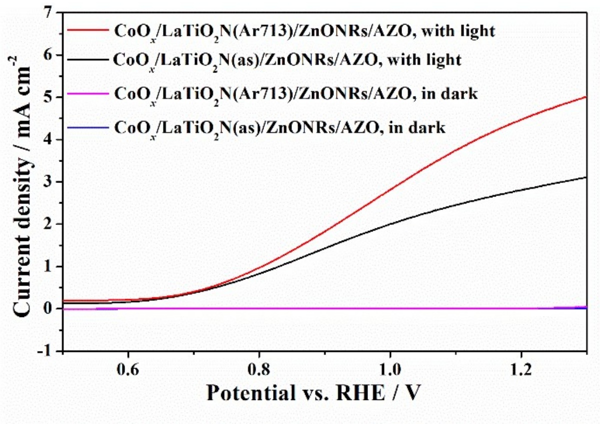

Fig. S3 Current-potential characteristics of photoanodes in 0.1 M NaOH + 0.1 M Na_2SO_3 under AM 1.5G irradiation or in dark

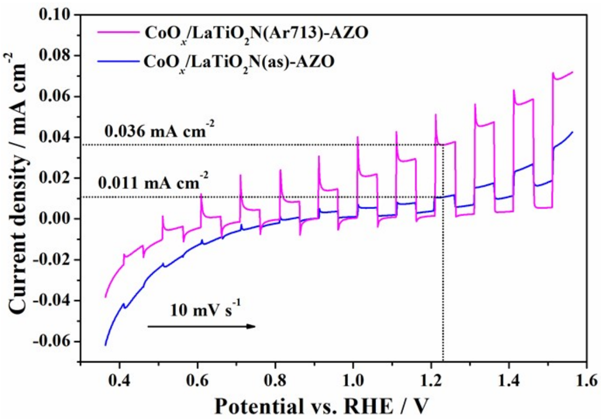

Fig. S4 Current-potential characteristics of photoanodes in 0.1 M NaOH under chopped AM 1.5G irradiation.

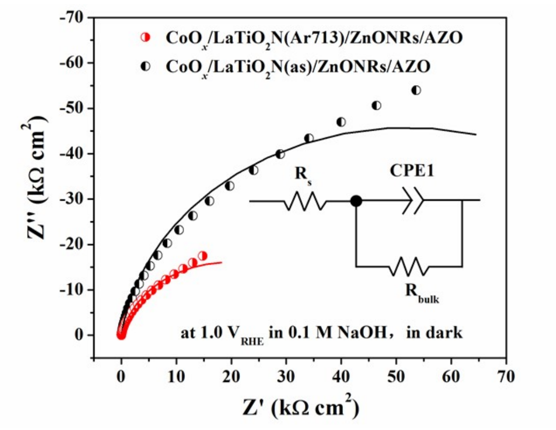

Fig. S5 Electrochemical impedance spectra of photoanodes in 0.1 M NaOH in dark. The dark impedances are very large at low frequencies, so the fitting errors are large, but the equivalent circuit can be used to fit well in the high-frequency region. It is shown that the bulk resistance of CoO_x/$LaTiO_2N$(Ar713)/ZnONRs/AZO electrode in dark is less than that of CoO_x/$LaTiO_2N$(as)/ZnONRs/AZO electrode (Table S3).

Table S1 Fitting parameters of EIS Nyquist curve for $CoO_x/LaTiO_2N$-AZO photoanodes under AM 1.5G irradiation

Element	Value	Error	Error%	Value	Error	Error%
	$CoO_x/LaTiO_2N$(as)-AZO			$CoO_x/LaTiO_2N$(Ar713)-AZO		
$R_s/\Omega\ cm^2$	13.9	0.0644	0.462	12.3	0.0769	0.624
CPE-T	2.14×10^{-5}	1.06×10^{-7}	0.494	1.17×10^{-5}	8.93×10^{-8}	0.761
CPE-P	0.899	9.36×10^{-4}	0.104	0.945	1.30×10^{-3}	0.139
$R_{bulk}/\Omega\ cm^2$	1.06×10^{5}	1.97×10^{3}	1.85	3.94×10^{4}	371	0.940

Table S2 Fitting parameters of EIS Nyquist curve for $CoO_x/LaTiO_2N$/ZnONRs/AZO photoanodes under AM 1.5G irradiation

Element	Value	Error	Error%	Value	Error	Error%
	$CoO_x/LaTiO_2N$(as)/ZnONRs/AZO			$CoO_x/LaTiO_2N$(Ar713)/ZnONRs/AZO		
$R_s/\Omega\ cm^2$	10.2	0.0166	0.163	10.4	0.0216	0.208
CPE2-T	9.18×10^{-5}	1.42×10^{-5}	1.54	1.58×10^{-4}	2.80×10^{-5}	1.77
CPE2-P	0.828	5.64×10^{-3}	0.681	0.871	5.61×10^{-3}	0.645
$R_{ct}/\Omega\ cm^2$	78.0	0.583	0.748	68.0	0.448	0.659
CPE1-T	8.09×10^{-5}	1.73×10^{-6}	2.14	4.08×10^{-4}	2.12×10^{-5}	5.19
CPE1-P	0.821	2.54×10^{-3}	0.310	0.761	6.56×10^{-3}	0.861
$R_{bulk}/\Omega\ cm^2$	53.4	0.422	0.789	19.7	0.357	1.81

Table S3 Fitting parameters of EIS Nyquist curve for $CoO_x/LaTiO_2N$/ZnORs/AZO photoanodes in dark

Element	Value	Error	Error%	Value	Error	Error%
	$CoO_x/LaTiO_2N$(as)/ZnONRs/AZO			$CoO_x/LaTiO_2N$(Ar713)/ZnONRs/AZO		
$R_s/\Omega\ cm^2$	10.4	0.0829	0.794	10.4	0.0484	0.464
CPE-T	2.70×10^{-5}	2.37×10^{-7}	0.879	1.15×10^{-4}	6.40×10^{-6}	0.558
CPE-P	0.918	1.74×10^{-3}	0.190	0.876	1.30×10^{-3}	0.148
$R_{bulk}/\Omega\ cm^2$	1.04×10^{5}	2.34×10^{3}	2.25	3.90×10^{4}	749	1.92